



Mycobacterium smegmatis GlnR Regulates the Glyoxylate Cycle and the Methylcitrate Cycle on Fatty Acid Metabolism by Repressing *icl* Transcription

Nan Qi¹, Guo-Lan She¹, Wei Du¹ and Bang-Ce Ye^{1,2*}

¹ Institute of Engineering Biology and Health, Collaborative Innovation Center of Yangtze River Delta Region Green Pharmaceuticals, College of Pharmaceutical Sciences, Zhejiang University of Technology, Hangzhou, China, ² Lab of Biosystems and Microanalysis, State Key Laboratory of Bioreactor Engineering, Institute of Engineering Biology and Health, East China University of Science and Technology, Shanghai, China

OPEN ACCESS

Edited by:

Haiké Antelmann,
Freie Universität Berlin, Germany

Reviewed by:

Ghader Bashiri,
The University of Auckland,
New Zealand
Jin Wang,
Chinese Academy of Sciences (CAS),
China
Agnese Serafini,
Independent Researcher, Rome, Italy

*Correspondence:

Bang-Ce Ye
bcye@ecust.edu.cn

Specialty section:

This article was submitted to
Microbial Physiology and Metabolism,
a section of the journal
Frontiers in Microbiology

Received: 08 September 2020

Accepted: 12 January 2021

Published: 03 February 2021

Citation:

Qi N, She G-L, Du W and Ye B-C
(2021) *Mycobacterium smegmatis*
GlnR Regulates the Glyoxylate Cycle
and the Methylcitrate Cycle on Fatty
Acid Metabolism by Repressing *icl*
Transcription.
Front. Microbiol. 12:603835.
doi: 10.3389/fmicb.2021.603835

Mycobacterium smegmatis (*Msm*), along with its pathogenic counterpart *Mycobacterium tuberculosis* (*Mtb*), utilizes fatty acids and cholesterol as important carbon and energy sources during the persistence within host cells. As a dual-functional enzyme in the glyoxylate cycle and the methylcitrate cycle, isocitrate lyase (ICL, encoded by *icl* or *MSMEG_0911*) is indispensable for the growth of *Msm* and *Mtb* on short-chain fatty acids. However, regulation of *icl* in mycobacteria in response to nutrient availability remains largely unknown. Here, we report that the global nitrogen metabolism regulator GlnR represses *icl* expression by binding to an atypical binding motif in the *icl* promoter region under nitrogen-limiting conditions. We further show that GlnR competes with PrpR, a transcriptional activator of *icl*, and dominantly occupies the co-binding motif in the *icl* promoter region. In the absence of GlnR or in response to the excess nitrogen condition, *Msm* cells elongate and exhibit robust growth on short-chain fatty acids due to the PrpR-mediated activation of *icl*, thereby inducing enhanced apoptosis in infected macrophages. Taken together, our findings reveal the GlnR-mediated repression of *icl* on fatty acid metabolism, which might be a general strategy of nutrient sensing and environmental adaptation employed by mycobacteria.

Keywords: *Mycobacterium*, fatty acid metabolism, glyoxylate cycle, methylcitrate cycle, transcriptional regulation

INTRODUCTION

Mycobacterium tuberculosis (*Mtb*) is the pathogenic agent of tuberculosis (TB) that causes the death of millions of people annually (Data from the WHO Global Tuberculosis Report). Due to the long latency period, high pathogenicity, and the emergence of multidrug-resistant *Mtb* strains (Lin and Flynn, 2010; Getahun et al., 2015), seeking more effective TB treatments is a challenging task for medical researchers. Recently, studies have been focusing on microbial nutrient sensing and metabolism to explore their physiological significance in *Mtb* lifecycle and pathogenesis. It was reported that the metabolic enzymes of *Mtb*, such as methylisocitrate lyase (MCL) and malate synthase (MA), are important for its pathogenicity and survival (Eoh and Rhee, 2014;

Puckett et al., 2017). Studies of the metabolic network in *Mtb* can help us to screen potential drug targets for TB treatment.

It is commonly accepted that *Mtb* utilize host-derived fatty acids as an important carbon source for bacterial growth and virulence (Munoz-Elias et al., 2006; Lovewell et al., 2016). Fatty acids are converted to acetyl-CoA (for even- and odd-chain fatty acids) and propionyl-CoA (for odd-chain fatty acids) by β -oxidation. Different enzymatic systems are involved in the conversion of acetate (an even-chain fatty acid) and propionate (an odd-chain fatty acid) to their CoA forms, acetyl-CoA and propionyl-CoA. Subsequently, acetyl-CoA is directed into the glyoxylate cycle, while propionyl-CoA is cyclically metabolized through the methylcitrate cycle in order to avoid the accumulation of toxic metabolic by-products (Munoz-Elias et al., 2006; Upton and McKinney, 2007). The first-step reaction of the glyoxylate cycle is catalyzed by the *icl*-encoded isocitrate lyase (ICL), which converts isocitrate into glyoxylate and succinate (Zu et al., 1999). In addition, ICL catalyzes another reaction producing succinate in the methylcitrate cycle, by using 2-methylisocitrate as the substrate. ICL thus plays a dual-role in the glyoxylate cycle and methylcitrate cycle essential for fatty acid metabolism in mycobacteria (Gould et al., 2006). The inability of *icl*-deficient *Mtb* to establish an infection in mice highlights the significance of ICL for pathogenesis (Munoz-Elias and McKinney, 2005). Recent studies have analyzed crystal structure of *Mtb* ICL and explored the potential of ICL as a target for the treatment of latent TB (Bhusal et al., 2017). Therefore, it is of great importance to investigate the regulation of *icl* and identify potential ICL inhibitors.

As a global response regulator, GlnR controls the transcription of genes involved in nitrogen and carbon metabolism for sensing different nutritional status in mycobacteria and other actinobacteria (Tiffert et al., 2008; Liao et al., 2015). For instance, genes encoding enzymes for ammonium assimilation (*glnII*, *gdhA*), nitrite reduction (*nirB*) and urea cleavage (*ureA*) are under transcriptional regulation by GlnR in *Streptomyces-coelicolor* (Tiffert et al., 2008; Pullan et al., 2011). Our previous studies have shown that GlnR regulates the methylcitrate cycle by inhibiting the transcription of *prpDBC* operon (*prpD* encode Methylcitrate dehydratase; *prpB* encode methylisocitrate lyase and *prpC* encode methylcitrate synthase) in *Mycobacterium smegmatis* (*Msm*), the non-pathogenic counterpart of *Mtb* (Liu et al., 2019). PrpR, a transcriptional activator of *iclI*, binds to the *prpDBC* promoter along with GlnR in *Msm* and *Mtb* (Paweł et al., 2012; Liu et al., 2019). However, whether *icl* is regulated by GlnR remains unknown. It is thus imperative to study if GlnR and PrpR co-regulate *icl*.

Here, we report the GlnR-mediated regulation of *icl* (also designed as *aceA* or *MSMEG_0911*) during *Msm* growth on fatty acids. We demonstrate that GlnR represses the transcription of *icl* and decreases the abundance of ICL products in the glyoxylate cycle and the methylcitrate cycle under nitrogen starvation condition, thereby impairing the growth, morphology and survival of *Msm* on short-chain fatty acids. Moreover, we unveil a competitive regulation of *icl* mediated by GlnR and PrpR, showing that GlnR blocks the PrpR-mediated activation of *icl* by occupying the co-binding motif in the promoter region.

Our findings thus reveal a regulatory role of GlnR on fatty acid metabolism by repressing *icl*, which might be a general strategy employed by mycobacteria in response to different nutrition status.

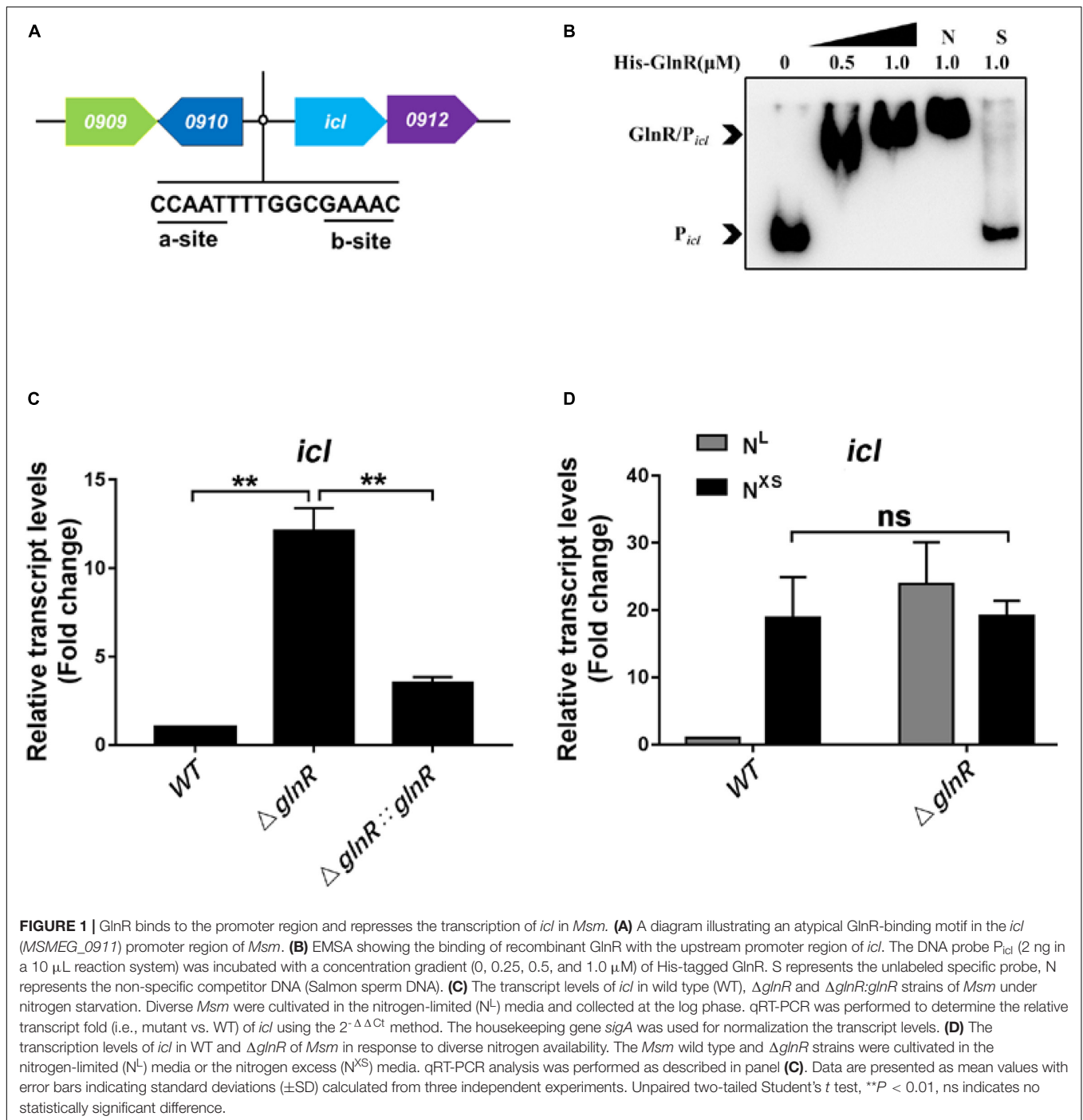
RESULTS

GlnR Represses the Transcription of *icl* in *Msm*

ICL is a dual-functional enzyme in the glyoxylate cycle and the methylcitrate cycle essential for the metabolism of fatty acids in *Msm* (Supplementary Figure S1). To study the regulation of *icl* by GlnR, we firstly searched for the GlnR-binding site in the promoter of *icl*. The classical binding framework of GlnR consists of two sites, a-site and b-site, separated by a hex-nucleotide motif (a-n6-b) (Fink et al., 2002; Tiffert et al., 2008; Liao et al., 2014). By sequence analysis using the Kyoto Encyclopedia of Genes and Genomes (KEGG) database and the Prokaryotic Operon database (ProOpDB)¹, we identified a putative binding site of GlnR (GlnR-box), -CCAATTTGGCGAAAC- at 300 bp upstream of the *icl* operon (Figure 1A). To further validate that GlnR could bind to the *icl* promoter region in *Msm*, recombinant His-tagged GlnR and biotin-labeled DNA probes containing the putative GlnR-box were subjected to the electrophoretic mobility shift assay (EMSA). Unlabeled specific probe (S) (200-fold excess) and non-specific competitor DNA (Salmon sperm DNA) (N) were used as controls. As shown in the Figure 1B, obvious shift bands were detected following the incubation of recombinant GlnR with the specific DNA probes, demonstrating that GlnR directly binds to the *icl* promoter region in *Msm*. To further validate the binding activity, we introduced loss-of-function mutations into the GlnR-binding motif as previously described (Jenkins et al., 2013). Mutation in the typical b-site (replacing -GAAAC- with -GAAGG-) completely abolished the binding of GlnR to the *icl* promoter (Supplementary Figure S2A). Notably, the a-site mutation (replacing -CCAAT- with -CCAGG-) in GlnR-box substantially attenuated the binding affinity of GlnR to the *icl* promoter, as we observed a faster electrophoretic mobility of GlnR-P_{icl} which is attributed to the less protein binding (Muller and Salles, 1997; Pham et al., 2004; Xu et al., 2019). These results suggest that both the typical b-site and the atypical a-site in GlnR-box of *icl* promoter are indispensable for GlnR binding. Furthermore, we detected a weak binding affinity between GlnR and the *Mtb icl* promoter (Supplementary Figures S2B,C), suggesting that the atypical GlnR-box might be conserved in the *icl* promoter in mycobacteria.

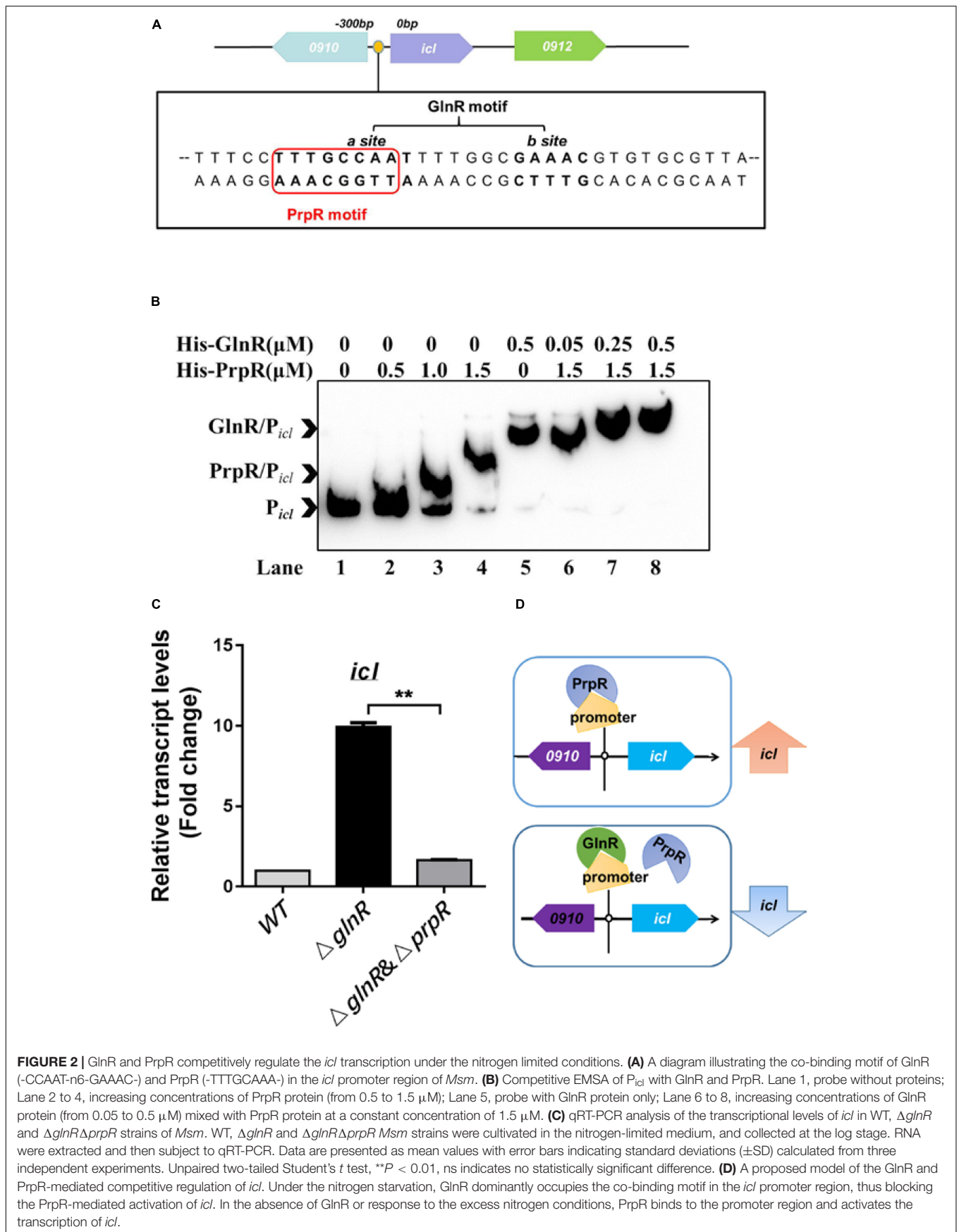
We next examined whether GlnR directly regulates the transcription of *icl* on fatty acid metabolism. To this end, *Msm* were cultured in minimal medium with propionate as the sole carbon source. Since the expression of *glnR* responses to the nitrogen starvation (Amon et al., 2008; Jenkins et al., 2013), we analyzed the differential transcription levels of *icl* among *Msm* wild type strain (WT), the *glnR*-deficient strain (Δ *glnR*) described previously (Liu et al., 2019), and the *glnR*

¹<http://www.ncbi.nlm.nih.gov/pmc/articles/PMC3245079/>



complemented strain (Δ *glnR::glnR*) under the nitrogen-limited (N^L , 1 mM ammonium sulfate) condition. Compared with WT *Msm*, the Δ *glnR* strain exhibited an increased *icl* transcript level, which returned to basal levels upon complementation by *glnR* (Figure 1C). It has been well-established that the *glnR* expression in WT *Msm* is completely blocked in response to the excess nitrogen (N^{XS} , 30 mM ammonium sulfate) condition (Xu et al., 2017). Under the N^{XS} condition, *icl* transcript levels dramatically increased in WT *Msm*, to reach

the same levels as in the Δ *glnR* strain (Figure 1D), further demonstrating that the down regulation of *icl* transcription is mediated by GlnR. Under the same conditions, GlnR had no impacts on the transcription of another ICL-encoding gene *MSMEG_3706* (Supplementary Figure S2D). Moreover, the repression of *icl* transcription by GlnR was validated when the carbon source propionate was replaced with other short-chain fatty acids like acetate, butyrate and valerate (Supplementary Figure S2E). We thus conclude that GlnR is a transcriptional



repressor of *icl* (*MSMEG_0911*) during *Msm* growth on short-chain fatty acids.

GlnR Blocks the PrpR-Mediated Activation of *icl*

It was previously reported that PrpR activates *icl1* transcription in *Mtb* and *Msm* (Pawel et al., 2012). In the *icl* promoter region, we noticed that a typical binding motif of PrpR (PrpR-box), -TTTGCAA-, is present in the GlnR-box (Figure 2A). All these findings inspired us to speculate that GlnR and PrpR coordinately regulate *icl* transcription in the methylcitrate cycle. To test this hypothesis, we performed competitive EMSA to examine whether GlnR and PrpR are competing with each other to bind to the probe P_{icl} , which is derived from the *icl* promoter containing both GlnR- and PrpR-box. As shown in Figure 2B, recombinant PrpR bound to P_{icl} , while an increasing dose of GlnR shifted the mobility of PrpR/ P_{icl} binding band to that of GlnR/ P_{icl} , indicating that GlnR dominates PrpR in competing for the *icl* promoter. In addition, we measured the affinity constants (KD values) of GlnR and PrpR for P_{icl} . The KD value of PrpR for P_{icl} is nearly 5-fold higher than the KD value of GlnR for P_{icl} (Supplementary Figures S3A,B), further demonstrating that GlnR has higher affinity for the *icl* promoter than PrpR.

To study the competitive effects of GlnR with PrpR on regulating *icl* transcription, we deleted *prpR* in the genome of the *Msm* Δ *glnR* strain, thereby generating the Δ *glnR* Δ *prpR* strain. We found that the transcriptional induction of *icl* caused by *glnR*-deficiency is attributed to the PrpR-mediated activation, as the increased mRNA level of *icl* in the Δ *glnR* strain was returned to basal level in the Δ *glnR* Δ *prpR* strain (Figure 2C, compare Δ *glnR* and Δ *glnR* Δ *prpR*). As illustrated in our proposed model (Figure 2D), these collective findings suggest that GlnR has a higher affinity to the shared region of *icl* promoter in comparison with PrpR, thus antagonizing the PrpR-mediated activation of *icl*.

GlnR Decreases the Cellular Concentrations of Intermediates in the Glyoxylate Cycle and the Methylcitrate Cycle During *Msm* Growth on Propionate

Given that the *icl* transcription is repressed by GlnR under nitrogen starvation, it is of interest to examine whether GlnR impairs the *icl*-encoded ICL enzyme activities. We thus used LC-MS to quantify the differential levels of ICL products in the glyoxylate and the methylcitrate cycles among diverse *Msm* strains during growth on propionate. The cellular concentrations of ICL-catalyzed products, glyoxylate and succinate, as well as the downstream intermediate malate, were increased in the Δ *glnR* strain during growth on propionate under the nitrogen-limited conditions (Figures 3A–C). However, this pronounced effect induced by the *glnR*-deletion was not detected under the excess nitrogen culture conditions. Together with the transcriptional analysis, these data suggest that the repression of *icl* expression by GlnR decreases the flux of ICL-catalyzed products through the glyoxylate cycle and methylcitrate cycle.

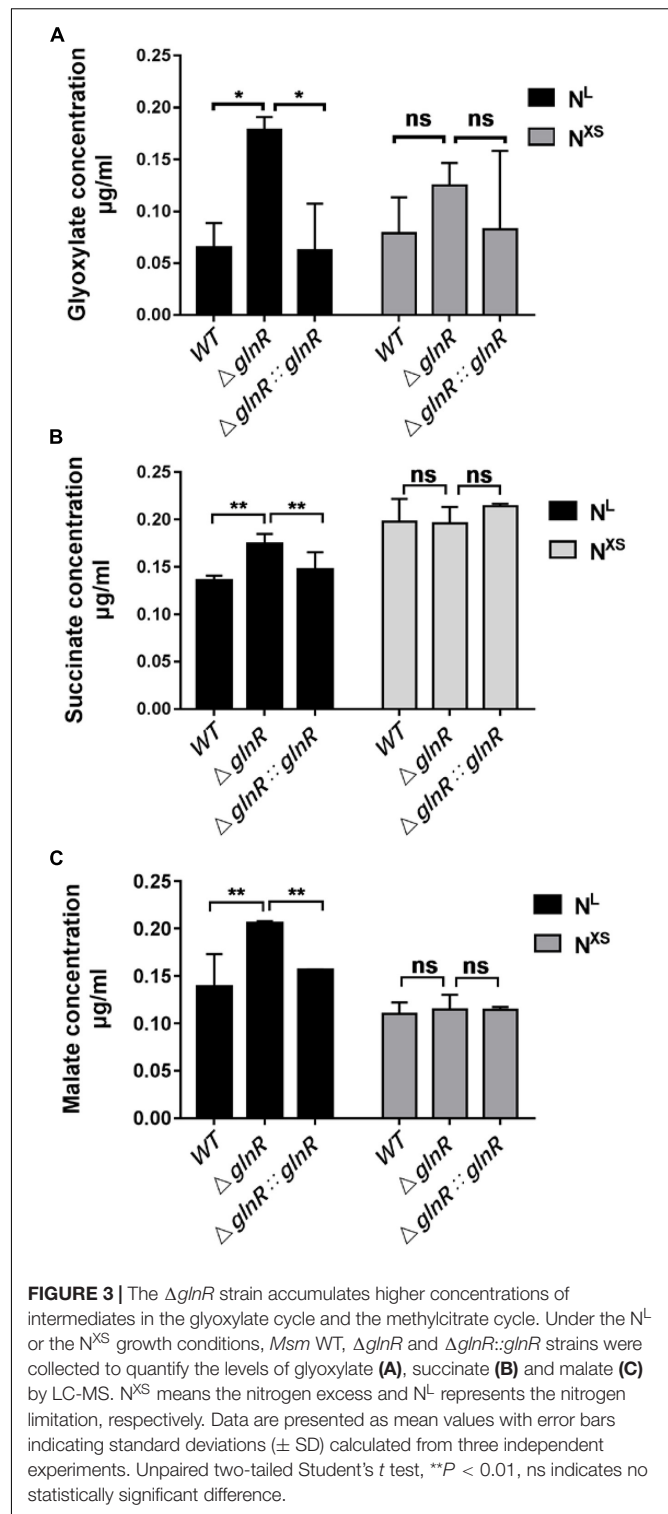


FIGURE 3 | The Δ *glnR* strain accumulates higher concentrations of intermediates in the glyoxylate cycle and the methylcitrate cycle. Under the N^L or the N^{XS} growth conditions, *Msm* WT, Δ *glnR* and Δ *glnR*::*glnR* strains were collected to quantify the levels of glyoxylate (A), succinate (B) and malate (C) by LC-MS. N^{XS} means the nitrogen excess and N^L represents the nitrogen limitation, respectively. Data are presented as mean values with error bars indicating standard deviations (\pm SD) calculated from three independent experiments. Unpaired two-tailed Student's *t* test, ***P* < 0.01, ns indicates no statistically significant difference.

GlnR Hinders the Growth and Cell Elongation of *Msm* on Short-Chain Fatty Acids

Having demonstrated that GlnR likely decreases flux through the glyoxylate cycle and methylcitrate cycle by transcriptionally

repressing the expression of *icl*, we next studied the physiological effects of GlnR-mediated down-regulation on *Msm* growth. For this purpose, the growth curves of various *Msm* strains were determined under diverse culture conditions. It was shown that the Δ *glnR* strain grows to higher final cell densities when using propionate or acetate as the sole carbon source, while this pronounced effect on growth were diminished by complementing with *glnR* or deleting *prpR* (Figures 4A,B). When glucose was the sole carbon source, no significant differences were observed among the growth curves of each strain (Figure 4C). We further observed the morphology of various *Msm* strains using scanning electron microscopy. Fifty cells were measured and calculated the average value for each strain. The average length of WT was $1.74 \pm 0.22 \mu\text{m}$; the (*glnR* strain was $2.33 \pm 0.05 \mu\text{m}$ and (*glnR::glnR* strain was $1.76 \pm 0.13 \mu\text{m}$. Notably, the *glnR*-deficiency resulted in an elongation of *Msm* cells when growing in propionate, as the cell length of (*glnR* strain were significantly longer than that of WT and the (*glnR::glnR* strain (Figures 4D,E and Supplementary Figure S4). An explanation is that the morphological elongation facilitates the Δ *glnR* strain to more efficiently absorb nutrients and grow better on the short-chain fatty acids. These findings thus establish GlnR as a negative effector on the growth of *Msm* in response to propionate.

Deletion of *glnR* Enhances the Apoptosis of Macrophages Infected With *Msm*

To study the physiological effects of GlnR-mediated regulation on *Msm* survival, THP-1-derived macrophages were infected with various *Msm* strains cultured on propionate. We used flow cytometry to measure the apoptosis rate of macrophages infected with mid-logarithmic ($\text{OD}_{600} = 0.4$) *Msm* at a multiplicity of infection (MOI) of 1, 5, or 10. To study if a release of metabolites from high amount of *Msm* would induce apoptosis, we performed comparison analysis between mutant and parental strains. Comparative experiments were also conducted using alive and killed bacteria. The Δ *glnR* strain consistently led to an enhanced apoptosis of *Msm*-infected macrophages at different MOI (Figures 5A,B). On the contrary, no difference was detected in the apoptosis rates of macrophages infected with killed bacteria (Supplementary Figure S5). These data indicate that the enhanced apoptosis induced by the Δ *glnR* strain is not related to the metabolites. Furthermore, we found that neither the proliferation of macrophages nor the survival of *Msm* in macrophages were impaired by deleting *glnR*, as no statistical difference was observed in the cell viability of macrophages or the survival rate of bacteria when comparing WT *Msm* and the Δ *glnR* strain (Figures 6A,B). Taken together, these results suggest that GlnR negatively impairs the apoptosis of macrophages infected with *Msm* which were pre-adapted to grow on propionate.

DISCUSSION

GlnR is a DNA-binding protein that regulates the transcription of genes related to nitrogen uptake and metabolism in both *Mtb* and *Msm* (Amon et al., 2008). Apart from nitrogen metabolism,

GlnR also controls the expression of genes involved in carbon metabolism. Our previous work reported that *Msm* GlnR affects the methylcitrate cycle through regulating the *prpDBC* operon by binding to the conserved motif GGACC-GGCACC-GTAAC (Liu et al., 2019). In this paper, we identified an atypical GlnR-binding motif, CCAAT-n6-GAAAC, in the promoter region of *icl* in *Msm*, and revealed that GlnR represses *icl* transcription. Moreover, we identified a GlnR-binding motif in upstream of the *icl* promoter in *Mtb*, and verified the binding of GlnR to P_{icl} by EMSA. Since *glnR* is highly conserved within the actinomycetes, future study is ongoing to test whether the GlnR-mediated regulation of *icl* is general in *Mtb* and other actinomycetes.

It was previously reported that PrpR directly activates the transcription of *icl1*, which encodes ICL involved in the glyoxylate cycle and methylcitrate pathways in both *Mtb* and *Msm* (Paweł et al., 2012). In our present work, PrpR is demonstrated to activate *icl* transcription in *Msm* once GlnR is absent or inactive under the excess nitrogen condition. A plausible explanation is that the higher binding affinity enables GlnR to occupy the promoter region of *icl* in competition with PrpR, thereby blocking the PrpR-mediated transcriptional activation of *icl*. We propose a model of the GlnR- and PrpR-mediated co-regulation of *icl* in fatty acid metabolism, which might be an adaptation strategy employed by mycobacteria in response to environmental nitrogen availability (Figure 7). In the evolutionary arms race between hosts and pathogens, host cells are able to antagonize *Mtb* by limiting the availability of amino acid such as aspartate, a major nitrogen source during *Mtb* infection (Shin et al., 2011; Zhang and Rubin, 2013). We speculate that *Mtb* adopts the GlnR-mediated regulatory mechanism to slow down its growth on host-derived fatty acid to adapt to the nitrogen-limited intracellular environment. At the late stage of infection, *Mtb* can synthesize its own amino acids and grow independently of the nitrogen-limited conditions in host cells (Zhang and Rubin, 2013). The nitrogen excess removes the GlnR-mediated repression of *icl* in *Mtb*, thus accelerating *Mtb* growth and enhancing the apoptosis of host cells. Therefore, our studies provide new insights into the host-pathogens interaction based on bacterial sensing and metabolism.

Recent studies have elucidated the carbon flux in *Mtb*, primarily focusing on those pathways responsible for the transformation of propionyl-CoA into intermediates of TCA cycle like succinate, malate and oxaloacetate (Savvi et al., 2008; Puckett et al., 2017). Detoxification of propionyl-CoA present on the operation of the methylcitrate cycle and the methylmalonyl cycle, or incorporation of the propionyl-CoA into methyl-branched lipids of host cells, enabling *Mtb* to utilize and produce energy for their pathogenesis (Lovewell et al., 2016; Puckett et al., 2017). Recent discoveries are establishing lactate and pyruvate as important energy and carbon sources for *Mtb*, and showing that they are assimilated by through glyoxylate shunt and methylcitrate cycle (Billig et al., 2017; Osada-Oka et al., 2019; Serafini et al., 2019). Interestingly, the methylcitrate cycle can operate in reverse as a pathway for the synthesis of propionyl-CoA. The fact that *Mtb* can use the methylcitrate and glyoxylate cycles to assimilate carbon sources different from beta-oxidation derived products suggests

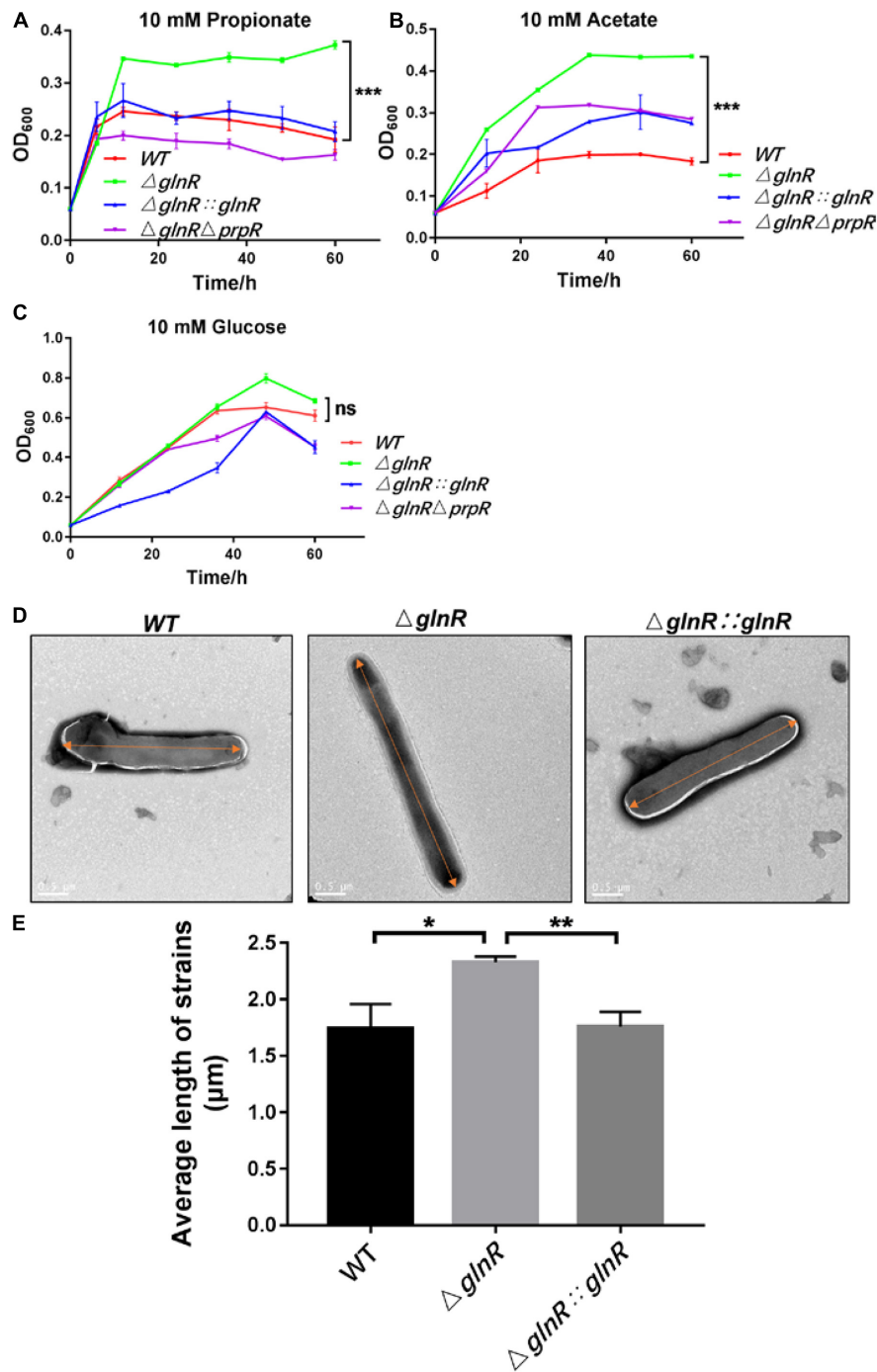


FIGURE 4 | The $\Delta glnR$ strain grows to higher optical densities and grows into elongated cells in response to short-chain fatty acids. The growth curves of *Msm* WT, $\Delta glnR$ and $\Delta glnR\Delta prpR$ strains growing in minimal medium with 10 mM propionate (A), acetate (B), glucose (C), respectively. Error bars represent the standard deviations from three biological replicates. (D,E) Deletion of *glnR* elongates bacteria cells during *Msm* growth on propionate. Scanning electron microscopy (SEM) images of bacteria cells from *Msm* WT, $\Delta glnR$ and $\Delta glnR\Delta prpR$ strains (D). Scale bar represents 0.5 μm . Length of bacteria cells ($n = 50$) was measured by manual evaluation, using Image J on the electron microscopic images (E). Data are presented as mean values with error bars indicating standard deviations (\pm SD) calculated from three independent experiments. Unpaired two-tailed Student's *t* test, * $P < 0.05$, ** $P < 0.01$, *** $P < 0.001$, ns indicates no statistically significant difference.

that GlnR might regulate these pathways independently from a certain carbon source including the short-chain fatty acids. In addition to the *icl* transcript levels, our present work also

explored the physiological effects of GlnR-mediated regulation on *Msm* survival, morphology and pathogenesis. Our data showed that the *glnR*-deficiency in *Msm* enables bacteria to grow to

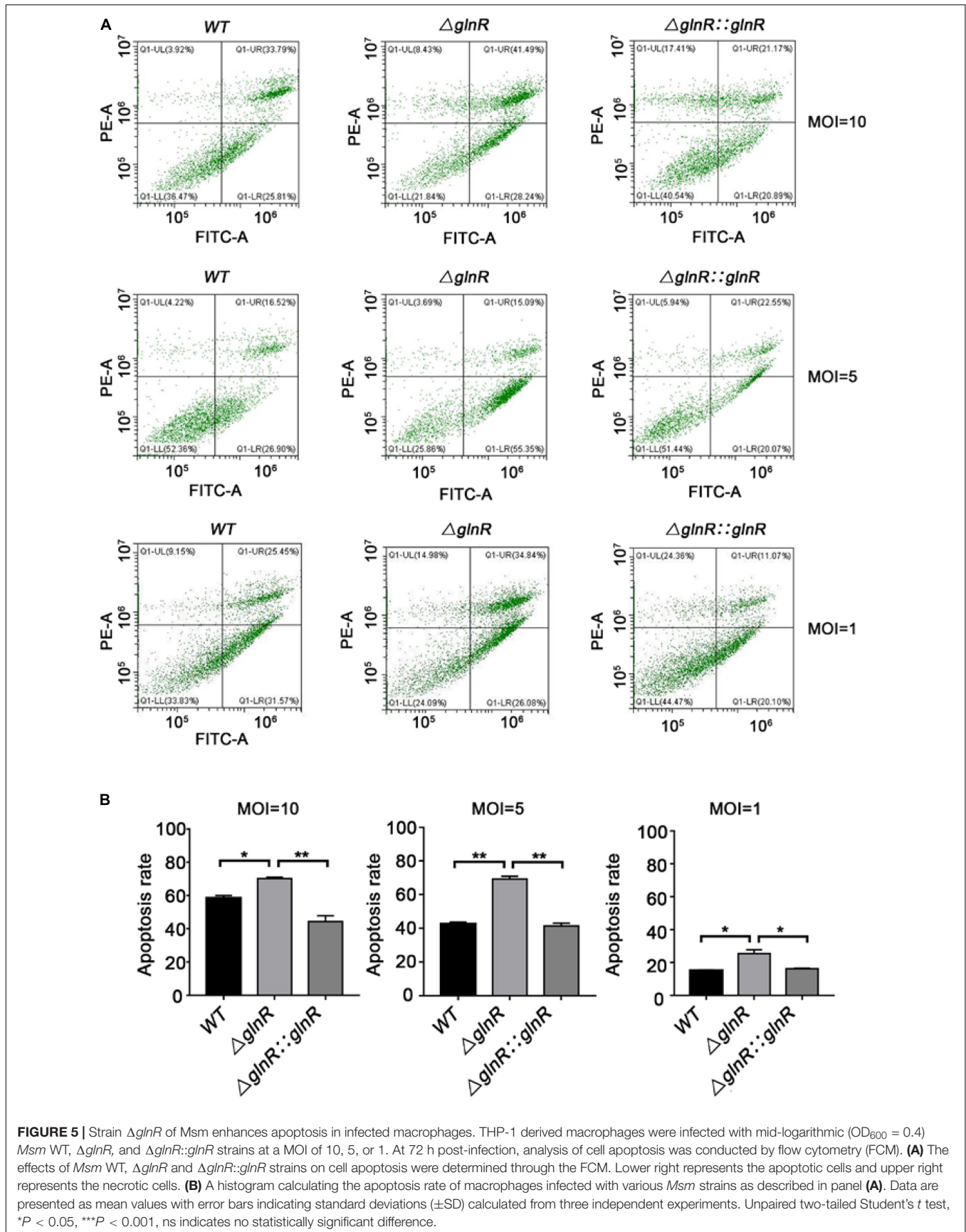


FIGURE 5 | Strain $\Delta glnR$ of *Msm* enhances apoptosis in infected macrophages. THP-1 derived macrophages were infected with mid-logarithmic ($OD_{600} = 0.4$) *Msm* WT, $\Delta glnR$, and $\Delta glnR::glnR$ strains at a MOI of 10, 5, or 1. At 72 h post-infection, analysis of cell apoptosis was conducted by flow cytometry (FCM). **(A)** The effects of *Msm* WT, $\Delta glnR$ and $\Delta glnR::glnR$ strains on cell apoptosis were determined through the FCM. Lower right represents the apoptotic cells and upper right represents the necrotic cells. **(B)** A histogram calculating the apoptosis rate of macrophages infected with various *Msm* strains as described in panel **(A)**. Data are presented as mean values with error bars indicating standard deviations (\pm SD) calculated from three independent experiments. Unpaired two-tailed Student's *t* test, **P* < 0.05, ****P* < 0.001, ns indicates no statistically significant difference.

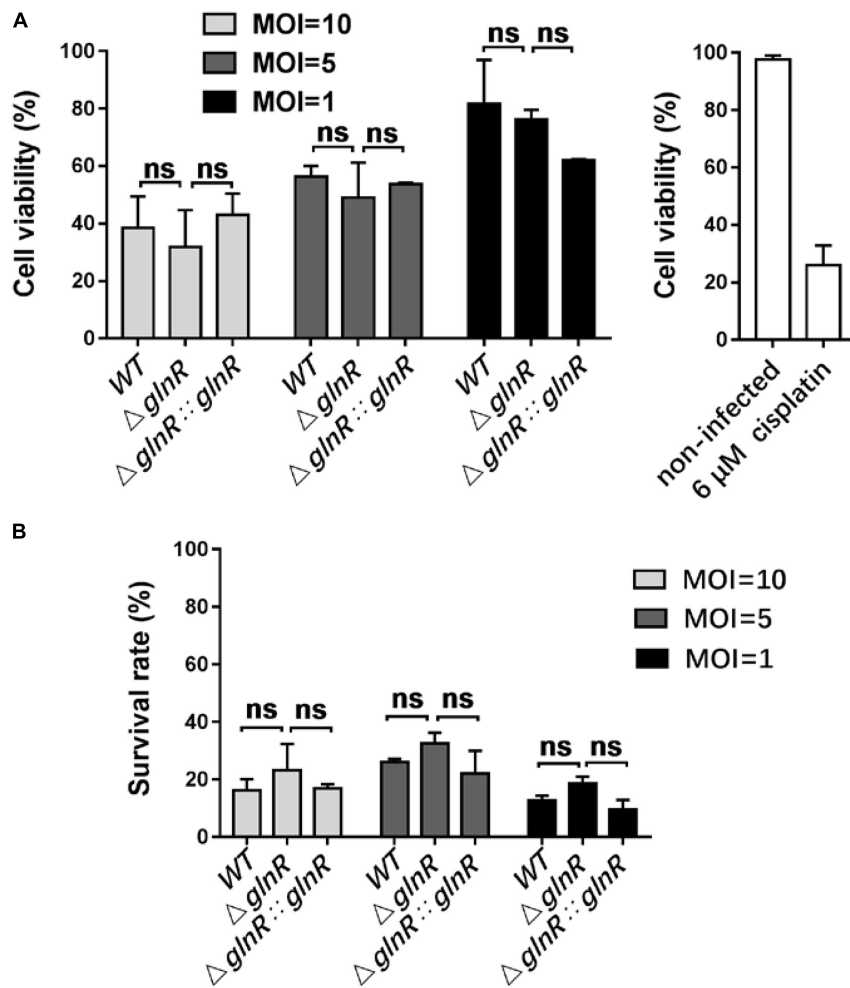
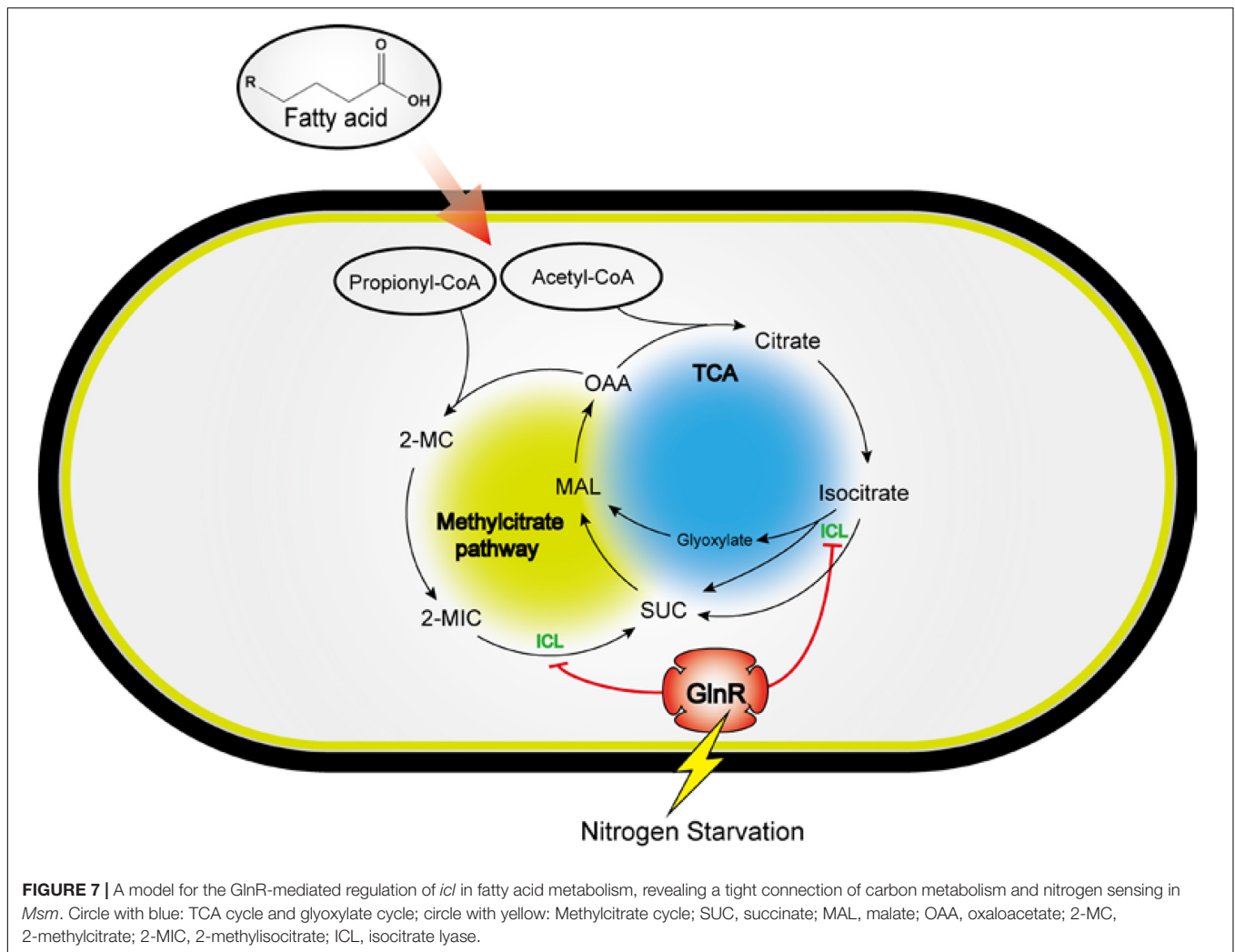


FIGURE 6 | Deletion of *glnR* in *Msm* has no impacts on the proliferation of infected macrophages and the survival of bacteria in macrophages. **(A)** Cell proliferation and viability of macrophages infected with *Msm* WT, $\Delta glnR$, and $\Delta glnR::glnR$ strains. Macrophages were infected with diverse *Msm* strains at MOI = 10, 5, 1, and subjected to MTT assay at 72 h post-infection. Cell viability (%) represents the ratio of OD₅₇₀ value of infected cells to that of non-infected cells. Cisplatin (6 μ M) was used as the positive control. **(B)** Survival of *Msm* WT, $\Delta glnR$, and $\Delta glnR::glnR$ strains in macrophages. At 0 or 72 h post-infection, bacteria in macrophages were collected for measuring the value of OD₆₀₀. Survival rate (%) represents the ratio of 72 h-OD₆₀₀ value to 0 h-OD₆₀₀ value. MOI = 10, 5, 1. Data are presented as mean values with error bars indicating standard deviations (\pm SD) calculated from three independent experiments. Unpaired two-tailed Student's *t* test, ns indicates no statistically significant difference.

higher final cell densities and trigger the cell elongation in response to short-chain fatty acids. The increased apoptosis of macrophages infected with *Msm* lacking GlnR was suspected to be connected to the role of GlnR in the regulation of certain metabolic pathways, as it is unknown which nutrient activates such pathways during infection. Here, we proposed two mechanistic hypotheses regarding why the $\Delta glnR$ strain has improved growth on propionate and was morphologically elongated in comparison with WT *Msm*: (1) Since the elevated ICL activities by *glnR*-deficiency accelerate the propionyl-CoA metabolism in the $\Delta glnR$ strain, the assimilation of propionyl-CoA and other toxic metabolites such as 2-methylcitrate are strengthened, posing a positive impact on the growth of *Msm* utilizing propionate as the sole carbon source. (2) Since the intermediate of propionyl-CoA metabolism, succinate, is also

linked to methylmalonyl-CoA metabolism, we speculated that increase of succinate in the $\Delta glnR$ strain would probably enhance the metabolic flux of methylmalonyl-CoA, which is coupled with the synthesis of lipids (PDIM and SL-1) in bacterial cell wall (Kumar et al., 2007). Owing to the accelerating synthesis of lipids in cell wall, the bacteria cells of *Msm* $\Delta glnR$ strain are elongated. Since *Msm* is not a host-adapted bacterium, the nutrient response of *Msm* might be different from that of *Mtb* adapting to the host intracellular environment. Studies based on a *Mtb*-infected mice model is imperative to elucidate the nutrient response of *Mtb* in macrophages, and further explore the physiological significance in the future.

ICL has emerged as a potential drug target for TB therapy. Currently, inhibitors of ICL, such as 3-nitropropionate, block *Mtb* growth in infected murine macrophages (McFadden, 1977;



Altaf et al., 2010). However, these chemicals are unsuitable for TB therapy due to their side effects inhibiting key metabolism enzymes activities of host. As revealed in our present work, GlnR is a repressor of *icl* and affects ICL production under the nitrogen-limited condition. Therefore, nutrient adjustment reducing nitrogen uptake might be a potential adjuvant treatment of TB, through the GlnR-mediated repression of ICL activities and *Mtb* persistence in host cells.

MATERIALS AND METHODS

Strains, Plasmids and Growth Conditions

Strains and plasmids used in this work were listed in Table 1. *E. coli* strains were grown at 37°C in liquid or on solid LB medium. *Msm* wild type, $\Delta glnR$, $\Delta glnR::glnR$ and $\Delta glnR\Delta prpR$ strains were cultivated on liquid LB medium which contains 0.05% tween-80. After being washed for three times with normal saline, the bacteria were incubated in nitrogen free Sauton's medium [0.05% (w/v) KH₂PO₄, 0.05% (w/v) MgSO₄, 0.2% (w/v) citric acid, 0.005% (w/v) ferric citrate, 0.2% (v/v)

glycerol, 0.0001% (v/v) ZnSO₄, 0.015% (v/v) Tyloxapol] (Jenkins et al., 2013) with 1 mM ammonium sulfate (N^L) or 30 mM ammonium sulfate (N^{XS}) and 10 mM sodium propionate used for transcription analysis, scanning electron microscopy analysis and mass spectrometry analysis, respectively. *Msm* wild type, $\Delta glnR$, $\Delta glnR::glnR$ and $\Delta glnR\Delta prpR$ strains were grown in M9 medium (Hayden et al., 2013; Liu et al., 2019) containing 10 mM glucose, 10 mM sodium acetate or 10 mM sodium propionate to measure the growth curve. All the strains were grown at 37°C and the medium were sterilized by autoclaving at 121°C for 20 min.

Construction of Deletion Mutant Strains

The gene knockout strategy was described in previous studies (Pelicic et al., 1997; Mathew et al., 2005). Briefly, a recombination cassette was constructed to delete *prpR* from the *Msm* $\Delta glnR$ chromosome. It consisted of a 1.3 kb DNA fragment on the upstream of *prpR* and a downstream fragment of DNA about 1.2 kb with the fragment holding the *kan* gene from plasmid PET-28a between them. After the preparative cloning steps, the whole recombination cassette was transferred to the suicide

TABLE 1 | Strains and plasmids used in this study.

Strains/plasmids	Source or Reference
<i>E. coli</i> BL21(DE3)	Novagen
<i>E. coli</i> DH5 α	Novagen
<i>Msm mc</i> ² 155	Dr. Brian D. Robertson gifted
<i>Msm mc</i> ² 155 Δ <i>glnR</i>	Dr. Brian D. Robertson gifted
<i>Msm mc</i> ² 155 Δ <i>glnR</i> Δ <i>glnR</i>	Constructed by our laboratory (Liu et al., 2019)
pET-28a	Novagen
pMV361- <i>glnR</i>	Constructed by our laboratory
pET-28a- <i>prpR</i>	Constructed by our laboratory
pET-28a- <i>glnR</i>	Constructed by our laboratory
pET-28a-Rv- <i>glnR</i>	Constructed by our laboratory
<i>Msm mc</i> ² 155 Δ <i>glnR</i> Δ <i>prpR</i>	In this work
pPR27	DipankarChatterji

vector pPR27 to get the final construct. The *sacB* mutant gentamicin-susceptible and kanamycin-resistant colonies were selected for further analysis. The selected mutants (Δ *glnR* Δ *prpR*) were verified by PCR and DNA sequencing. Sequences of primers were shown as in Table 2.

Protein Expression and Purification in *E. coli* BL21 (DE3)

The protein His-GlnR, His-PrpR and His-Rv-GlnR were expressed in *E. coli* BL21 (DE3) strains which was constructed in our previous work, strains were cultured in 5 ml LB (0.05 mg/ml kanamycin) overnight, and then transferred to 50 ml LB (0.05 mg/ml kanamycin). A total of 0.7 mM isopropyl- β -D- thiogalactopyranoside was added when the optical density at 600 nm (OD₆₀₀) of the cells was about 0.6. Then, the cells were grown at 20°C overnight (Yao and Ye, 2016; Liu et al., 2019). The purified proteins were assessed by sodium dodecyl sulfate-polyacrylamide gel electrophoresis, and protein concentration was determined using the Bradford reagent.

Electrophoretic Mobility Shift Assay (EMSA)

The upstream regions (−300 to +50) of *icl* (*MSMEG_0911*) was amplified by PCR using gene-specific primers containing the universal primer (5′-AGCCAGTGGCGATAAG-3′) sequence (Table 2) and biotin labeled by PCR using the 5′ biotin-modified universal primer. The PCR products were analyzed by agarose gel electrophoresis and purified using a gel extraction kit (Transgen Biotech Co., Ltd., Beijing, China). The concentration of biotin-labeled DNA probes was determined using a microplate reader (BioTek, United States). The next steps were the same as our previous work (Xu et al., 2016; Yao and Ye, 2016; Liu et al., 2019). EMSAs were carried out according to manufacturer protocol for the chemiluminescent EMSA kit (Beyotime Biotechnology, Jiangsu, China).

Quantitative Real-Time PCR

Cells at exponential stage in nitrogen-limited medium were collected by centrifugation. Total RNA was prepared using an

RNeasy mini kit (Qiagen, Valencia, CA, United States). The RNA quality was analyzed by 1% agarose gel electrophoresis, and the concentration was determined by microplate reader (BioTek, United States). The RNA was reverse transcribed to cDNA using a PrimeScript reverse transcription (RT) reagent kit with gDNA Eraser (TaKaRa, Shiga, Japan), and DNase digestion was performed to remove genomic DNA before reverse transcription for 5 min at 42°C. The RT-PCR was performed with primers listed in Table 2 and performed in a 20 μ L PCR solution from the SYBR premix Ex Taq GC kit (Perfect Real Time; TaKaRa, Japan) using about 100 ng cDNA as the template. All procedures were performed according to the manufacturer's instructions. PCR was conducted using a CFX96 real-time system (Bio-Rad, Hercules, CA, United States) with PCR conditions of 95°C for 5 min, then 40 cycles at 95°C for 5 s and 60°C for 30 s, and an extension at 72°C for 10 min, same as our previous study (You et al., 2017). Data was normalized by the level of housekeeping gene *sigA* in each individual sample. The relative transcript levels of target gene were calculated using the $2^{-\Delta\Delta Ct}$ method.

Determination of Affinity Constant (KD Value)

The binding affinities of GlnR and PrpR proteins to the upstream region of the *icl* operon were determined by Bio-Layer interferometry using an Octet System (Octet QKe; ForteBio, United States). Streptavidin biosensors were loaded with biotinylated DNA fragment (upstream region of *icl*) by incubation for 5 min in 7 μ g/ml DNA solution (containing 10 mM HEPES, 2 mM magnesium chloride, 0.1 mM EDTA, 200 mM potassium chloride, pH 8.0), and then washed in loading buffer for 5 min. After that, the biosensors were moved to protein solutions to allow association for 10 min, and then transferred into running buffer (containing 10 mM HEPES, 2 mM magnesium chloride, 0.1 mM EDTA, 200 mM potassium chloride, 10 μ g/ml bovine serum albumin, 0.02% Tween-20, pH 8.0) to detect dissociation. All incubations were performed in a 96-well plate at 37°C at 1,000 rpm in a volume of 100 μ L. The kinetic parameters K_{on} , K_{off} , and KD were calculated by 1:1 binding model using the Octet Data Analysis version 7.0.

Scanning Electron Microscopy (SEM) Analysis

Strains were cultivated to log phase and harvested in 4°C with centrifuge of 6000 \times g, washed twice and resuspended with normal saline. Strains were stained with 2% phosphotungstic acid and after 2 min later, analyzed the morphology of bacterial by JEM-4100. Length of bacteria was analyzed by manual evaluation, using Image J on the electron microscopic images.

Liquid Chromatography-Mass Spectrometry (LC-MS) Analysis

Bacteria were cultured to log phase in Sauton's medium with 10 mM sodium propionate under the N^L (1 mM ammonium sulfate) or the N^{XS} (30 mM ammonium sulfate) conditions,

TABLE 2 | List of primers used in this study.

Name	Sequence (5' → 3')	purpose
MSM6643- UP-F	GAATTGGAGCTCCACCGCGGTGGCGGCCAGTTCGATGGTGTCCGGTCCGGTGC	amplification of Msmeg_6643 upstream fragment
MSM6643- UP-R	CAAGACGTTTCCCCTTGAATATGGCTCATAACACAGCCCTAACCGCGATTCTTACACAG	amplification of Msmeg_6643 upstream fragment
Kan-F	CTGTGTAAGAATCGCGGTTAGGCTGTGTGTATGAGCCATATCAACGGGAAACGTCTTG	amplification of Kanamycin encodes genes
Kan-R	GGCGGCACTGATCAGCGGGGTCGTTGATTAGAAAACTCATCGAGCATCAAATG	amplification of Kanamycin encodes genes
MSM6643- DOWN-F	CATTTGATGCTCGATGAGTTTTTCTAATCAACGACCCCGCTGATCAGTGCCGCC	amplification of Msmeg_6643 downstream fragment
MSM6643- DOWN-R	GTGAGGATCGGGGATCCACTAGTTCTAGAGGCACTTCGGGTGTTCAAGGCCATC	amplification of Msmeg_6643 downstream fragment
MSM6643- DE-F	CCAGGGTGACGAACCTTGTTC	verify the deletion of Msmeg_6643
MSM6643- DE-R	CTCGCATCAACCAAACCGTTATTCA	verify the deletion of Msmeg_6643
Msmeg_0911_S	AGCCAGTGGCGATAAG ATATGCGGTGGCGAGGAGAC	amplification of Msmeg_0911 upstream regions
Msmeg_0911_A	AGCCAGTGGCGATAAG GTTGTGATCCAGTCGTGCTGGATC	amplification of Msmeg_0911 upstream regions
Universal primer	biotin-AGCCAGTGGCGATAAG	amplification of Msmeg_0911 upstream regions
MSM5784RT-F	GCGTAGATGGCTGCTCCGAAAT	used for Q-RT-PCR
MSM5784RT-R	CGCAGACTGGTGGTCGGGTT	used for Q-RT-PCR
MSM6643RT-F	CACCATCTCCTCGACATCGG	used for Q-RT-PCR
MSM6643RT-R	CAGGCTCTTACGTGCCATTAG	used for Q-RT-PCR
MSM0911RT-F	CCTCGAGAAGAAGTGCGGC	used for Q-RT-PCR
MSM0911RT-R	GAGGTCAGGGTGCGGATGTG	used for Q-RT-PCR

Sequences of each primer in 5' to 3' are given. The purpose of each oligo in this study is also mentioned.

collected by centrifugation and then frozen in liquid nitrogen for 1 min. After being restored to the room temperature, bacteria cells were treated with 75% boiling ethanol, heated in boiling water for 5 min, and then frozen at -80°C . Followed by high speed centrifugation, supernatants containing the intracellular organic acids were collected. Samples were subsequently concentrated by vacuum concentrator for LC-MS detection. Metabolites were separated on a ZORBAX Eclipse XDB-C18 column (4.6×250 mm, $5 \mu\text{m}$) at 30°C , the mass spectrometer used was an Agilent Accurate Mass 6530 Q-TOF coupled to an Agilent 1260 LC system. For elution, 1% (v/v) methanol (solvent A) and acetonitrile (solvent B) were used as the mobile phases at a flow rate of 1 mL/min. Data was analyzed by the "Q-TOF Quantitative Analysis." Calibration curves were performed by serial dilutions for different organic acid's standards to test correlation between chromatogram peaks areas and analyte quantities. All samples were analyzed in triplicate and results were reported as the average with standard deviation.

Cell Culture, Infection and Assessment of Cell Death

THP-1 cells were grown in RPMI 1640 (Gibco) supplemented with 10% fetal bovine serum (FBS; Gibco), 1% penicillin and streptomycin (Gibco). The cells were seeded onto 12-well culture dishes at a density of 2×10^5 cells ml^{-1} and treated overnight with 10 ng/ml phorbol myristate acetate (Sigma). Cells were washed three times with phosphate buffer saline and incubated for one more day, then infected with Msm wild type, ΔglnR , $\Delta\text{glnR}::\text{glnR}$ strains (killed bacteria as control) for 2 h with MOI at 10, 5, and 1 (strains were washed three times with normal saline). The infected cells were washed three times with RPMI 1640 medium to eliminate the suspended bacteria and then incubated in fresh RPMI 1640 medium with 15 $\mu\text{g}/\text{ml}$ gentamicin for 72 h. Annexin V-FITC&PI Apoptosis Detection Kit (Sangon

Biotech, China) was used according to the protocol in order to mark apoptotic THP-1 cells. Stained cells were analyzed immediately on CytoFlex (BECKMAN COULTER) and further analyzed with CytExpert.

MTT Assay

THP-1 cells (5×10^4 cells ml^{-1}) were seeded in a 96-well plate in triplicate and incubated for 12 h for cell attachment, replace a new medium, after 12 h added the Msm wild type, ΔglnR , $\Delta\text{glnR}::\text{glnR}$ strains with MOI at 10,5,1 into the 96-well plate. At 72 h post-infection, MTT [3-(4,5-Dimethylthiazol-2-yl)-2,5-Diphenyltetrazolium Bromide] solution was added to the 96-well plate and incubated for 4 h at 37°C , add the Formazan solution slowly and then continue incubation about 4 h. OD₅₇₀ values were measured in a microplate reader (Synergy H1, Biotek).

Survival of Msm in Macrophages

THP-1 cells were divided into 12-well plates (2.0×10^5 cells ml^{-1}) and differentiated using phorbol myristate acetate when the cells were at the best state (He et al., 2017). After 12 h, the cells were washed and then cultured in fresh RPMI 1640 medium for 12 h. The Msm wild type, ΔglnR , $\Delta\text{glnR}::\text{glnR}$ strains were added into the plates (10 times more than the macrophage cells), with MOI at 10, 5, 1. After incubating for 2 h, the cells were washed three times using fresh medium to remove the uninfected bacteria. The infected cells were cultured in fresh medium with gentamicin. After 72 h, the cells were washed three times with fresh medium, and then LB medium containing 0.05% SDS was added to lyse the cells for 10 min. The lysates were collected and diluted at different gradients to the inoculate plate. The Msm colony-forming units were counted after 3 days of culturing (Tiffert et al., 2008).

DATA AVAILABILITY STATEMENT

The original data presented in the study are included in the article/**Supplementary Material**, further inquiries can be directed to the corresponding author/s.

AUTHOR CONTRIBUTIONS

NQ and G-LS was responsible for experimental design, data collection, and writing manuscript. WD participated in plasmid construction and HPLC analysis. B-CY was responsible for experimental design, data analysis, and final approval of the manuscript. All authors contributed to the article and approved the submitted version.

REFERENCES

- Altamirano, M., Miller, C. H., Bellows, D. S., and O'Toole, R. (2010). Evaluation of the *Mycobacterium smegmatis* and BCG models for the discovery of *Mycobacterium tuberculosis* inhibitors. *Tuberculosis (Edinb)* 90, 333–337. doi: 10.1016/j.tube.2010.09.002
- Amon, J., Bräu, T., Grimrath, A., Hänsler, E., Hasselt, K., Höller, M., et al. (2008). Nitrogen control in *Mycobacterium smegmatis*: nitrogen-dependent expression of ammonium transport and assimilation proteins depends on the OmpR-type regulator GlnR. *J. Bacteriol.* 190, 7108–7116.
- Bhusal, R. P., Bashiri, G., Kwai, B. X. C., Sperry, J., and Leung, I. K. H. (2017). Targeting isocitrate lyase for the treatment of latent tuberculosis. *Drug Discov. Today* 22, 1008–1016. doi: 10.1016/j.drudis.2017.04.012
- Billig, S., Schneefeld, M., Huber, C., Grassl, G. A., Eisenreich, W., and Bange, F. C. (2017). Lactate oxidation facilitates growth of *Mycobacterium tuberculosis* in human macrophages. *Sci. Rep.* 7:6484. doi: 10.1038/s41598-017-05916-7
- Eoh, H., and Rhee, K. Y. (2014). Methylcitrate cycle defines the bactericidal essentiality of isocitrate lyase for survival of *Mycobacterium tuberculosis* on fatty acids. *Proc. Natl. Acad. Sci. U.S.A.* 111, 4976–4981. doi: 10.1073/pnas.1400390111
- Fink, D., Weißschuh, N., Reuther, J., Wohlleben, W., and Engels, A. (2002). Two transcriptional regulators GlnR and GlnRII are involved in regulation of nitrogen metabolism in *Streptomyces coelicolor* A3(2). *Mol. Microbiol.* 46, 331–347.
- Getahun, H., Matteelli, A., Chaisson, R. E., and Ravignone, M. (2015). Latent *Mycobacterium tuberculosis* infection. *New Engl. J. Med.* 372, 2127–2135. doi: 10.1056/NEJMra1405427
- Gould, T. A., van de Langemheen, H., Munoz-Elias, E. J., McKinney, J. D., and Sacchettini, J. C. (2006). Dual role of isocitrate lyase 1 in the glyoxylate and methylcitrate cycles in *Mycobacterium tuberculosis*. *Mol. Microbiol.* 61, 940–947. doi: 10.1111/j.1365-2958.2006.05297.x
- Hayden, J. D., Brown, L. R., Gunawardena, H. P., Perkowski, E. F., Chen, X., and Braunstein, M. (2013). Reversible acetylation regulates acetate and propionate metabolism in *Mycobacterium smegmatis*. *Microbiology* 159(Pt 9), 1986–1999. doi: 10.1099/mic.0.068585-0
- He, X., Jiang, H.-w., Chen, H., Zhang, H.-n., Liu, Y., Xu, Z.-w., et al. (2017). Systematic identification of *Mycobacterium tuberculosis* effectors reveals that BfrB suppresses innate immunity. *Mol. Cell. Proteom.* 16, 2243–2253. doi: 10.1074/mcp.RA117.000296
- Jenkins, V. A., Barton, G. R., Robertson, B. D., and Williams, K. J. (2013). Genome wide analysis of the complete GlnR nitrogen-response regulon in *Mycobacterium smegmatis*. *BMC Genom.* 14:301. doi: 10.1186/1471-2164-14-301
- Kumar, P., Schelle, M. W., Jain, M., Lin, F. L., Petzold, C. J., Leavell, M. D., et al. (2007). PapA1 and PapA2 are acyltransferases essential for the biosynthesis of the *Mycobacterium tuberculosis* virulence factor Sulfolipid-1. *Proc. Natl. Acad. Sci. USA* 104, 11221–11226. doi: 10.1073/pnas.0611649104

FUNDING

This work was supported by grants from the National Key Research and Development Project (2018YFA0900404), National Natural Science Foundation of China (31730004 to B-CY and 31870864 to NQ), and Fundamental Research Funds for the Provincial Universities of Zhejiang (RF-B2020003).

SUPPLEMENTARY MATERIAL

The Supplementary Material for this article can be found online at: <https://www.frontiersin.org/articles/10.3389/fmicb.2021.603835/full#supplementary-material>

- Liao, C. H., Yao, L., Xu, Y., Liu, W. B., Zhou, Y., and Ye, B. C. (2015). Nitrogen regulator GlnR controls uptake and utilization of non-phosphotransferase-system carbon sources in actinomycetes. *Proc. Natl. Acad. Sci. U.S.A.* 112, 15630–15635. doi: 10.1073/pnas.1508465112
- Liao, C. H., Yao, L. L., and Ye, B. C. (2014). Three genes encoding citrate synthases in *Saccharopolyspora erythraea* are regulated by the global nutrient-sensing regulators GlnR, DasR, and CRP. *Mol. Microbiol.* 94, 1065–1084.
- Lin, P. L., and Flynn, J. L. (2010). Understanding latent tuberculosis: a moving target. *J. Immunol.* 185, 15–22. doi: 10.4049/jimmunol.0903856
- Liu, W. B., Liu, X. X., Shen, M. J., She, G. L., and Ye, B. C. (2019). The nitrogen regulator GlnR directly controls transcription of the prpDBC operon involved in methylcitrate cycle in *Mycobacterium smegmatis*. *J. Bacteriol.* 201:e0099-19. doi: 10.1128/jb.00999-19
- Lovewell, R. R., Sassetti, C. M., and VanderVen, B. C. (2016). Chewing the fat: lipid metabolism and homeostasis during *M. tuberculosis* infection. *Curr. Opin. Microbiol.* 29, 30–36. doi: 10.1016/j.mib.2015.10.002
- Mathew, R., Ramakanth, M., and Chatterji, D. (2005). Deletion of the gene rpoZ, encoding the omega subunit of RNA polymerase, in *Mycobacterium smegmatis* results in fragmentation of the beta' subunit in the enzyme assembly. *J. Bacteriol.* 187, 6565–6570. doi: 10.1128/JB.187.18.6565-6570.2005
- McFadden, B. A. P. S. (1977). Itaconate, an isocitrate lyase-directed inhibitor in *Pseudomonas indigofera*. *J. Bacteriol.* 131, 136–144.
- Muller, C., and Salles, B. (1997). Regulation of DNA-dependent protein kinase activity in leukemic cells. *Oncogene* 15, 2343–2348. doi: 10.1038/sj.onc.1201402
- Munoz-Elias, E. J., and McKinney, J. D. (2005). *Mycobacterium tuberculosis* isocitrate lyases 1 and 2 are jointly required for in vivo growth and virulence. *Nat. Med.* 11, 638–644. doi: 10.1038/nm1252
- Munoz-Elias, E. J., Upton, A. M., Cherian, J., and McKinney, J. D. (2006). Role of the methylcitrate cycle in *Mycobacterium tuberculosis* metabolism, intracellular growth, and virulence. *Mol. Microbiol.* 60, 1109–1122. doi: 10.1111/j.1365-2958.2006.05155.x
- Osada-Oka, M., Goda, N., Saiga, H., Yamamoto, M., Takeda, K., Ozeki, Y., et al. (2019). Metabolic adaptation to glycolysis is a basic defense mechanism of macrophages for *Mycobacterium tuberculosis* infection. *Int. Immunol.* 31, 781–793. doi: 10.1093/intimm/dxz048
- Pawel, M., Anna, B., Marcin, W., Jarosław, D., and Jolanta, Z. C. (2012). A novel role of the PrpR as a transcription factor involved in the regulation of methylcitrate pathway in *Mycobacterium tuberculosis*. *PLoS One* 7:e43651. doi: 10.1371/journal.pone.0043651
- Pellicci, V., Jackson, M., Reyrat, J. M., Jacobs, W. R. Jr., Gicquel, B., and Guilhot, C. (1997). Efficient allelic exchange and transposon mutagenesis in *Mycobacterium tuberculosis*. *Proc. Natl. Acad. Sci. U.S.A.* 94, 10955–10960. doi: 10.1073/pnas.94.20.10955
- Pham, J. W., Pellino, J. L., Lee, Y. S., Carthew, R. W., and Sontheimer, E. J. (2004). A Dicer-2-dependent 80s complex cleaves targeted mRNAs during RNAi in *Drosophila*. *Cell* 117, 83–94. doi: 10.1016/s0092-8674(04)00258-2

- Puckett, S., Trujillo, C., Wang, Z., Eoh, H., Ioerger, T. R., Krieger, I., et al. (2017). Glyoxylate detoxification is an essential function of malate synthase required for carbon assimilation in *Mycobacterium tuberculosis*. *Proc. Natl. Acad. Sci. U.S.A.* 114, E2225–E2232. doi: 10.1073/pnas.1617655114
- Pullan, S. T., Chandra, G., Bibb, M. J., and Merrick, M. (2011). Genome-wide analysis of the role of GlnR in *Streptomyces venezuelae* provides new insights into global nitrogen regulation in actinomycetes. *BMC Genom.* 12:175.
- Savvi, S., Warner, D. F., Kana, B. D., McKinney, J. D., Mizrahi, V., and Dawes, S. S. (2008). Functional characterization of a vitamin B12-dependent methylmalonyl pathway in *Mycobacterium tuberculosis*: implications for propionate metabolism during growth on fatty acids. *J. Bacteriol.* 190, 3886–3895. doi: 10.1128/JB.01767-07
- Serafini, A., Tan, L., Horswell, S., Howell, S., Greenwood, D. J., Hunt, D. M., et al. (2019). *Mycobacterium tuberculosis* requires glyoxylate shunt and reverse methylcitrate cycle for lactate and pyruvate metabolism. *Mol. Microbiol.* 112, 1284–1307. doi: 10.1111/mmi.14362
- Shin, J. H., Yang, J. Y., Jeon, B. Y., Yoon, Y. J., Cho, S. N., Kang, Y. H., et al. (2011). (1)H NMR-based metabolomic profiling in mice infected with *Mycobacterium tuberculosis*. *J. Proteome Res.* 10, 2238–2247. doi: 10.1021/pr101054m
- Tiffert, Y., Supra, P., Wurm, R., Wohlleben, W., Wagner, R., and Reuther, J. (2008). The *Streptomyces coelicolor* GlnR regulon: identification of new GlnR targets and evidence for a central role of GlnR in nitrogen metabolism in actinomycetes. *Mol. Microbiol.* 67, 861–880.
- Upton, A. M., and McKinney, J. D. (2007). Role of the methylcitrate cycle in propionate metabolism and detoxification in *Mycobacterium smegmatis*. *Microbiology* 153(Pt 12), 3973–3982. doi: 10.1099/mic.0.2007/011726-0
- Xu, Y., Liao, C. H., Yao, L. L., Ye, X., and Ye, B. C. (2016). GlnR and PhoP Directly regulate the transcription of genes encoding starch-degrading, amylolytic enzymes in *Saccharopolyspora erythraea*. *Appl. Environ. Microbiol.* 82, 6819–6830. doi: 10.1128/AEM.02117-16
- Xu, Y., You, D., and Ye, B. C. (2017). Nitrogen regulator GlnR directly controls transcription of genes encoding lysine deacetylases in Actinobacteria. *Microbiology* 163, 1702–1710. doi: 10.1099/mic.0.000553
- Xu, Z., You, D., Tang, L. Y., Zhou, Y., and Ye, B. C. (2019). Metabolic engineering strategies based on secondary messengers (p)ppGpp and C-di-GMP to increase erythromycin yield in *Saccharopolyspora erythraea*. *ACS Synth. Biol.* 8, 332–345. doi: 10.1021/acssynbio.8b00372
- Yao, L. L., and Ye, B. C. (2016). Reciprocal regulation of GlnR and PhoP in Response to nitrogen and phosphate limitations in *Saccharopolyspora erythraea*. *Appl. Environ. Microbiol.* 82, 409–420. doi: 10.1128/AEM.02960-15
- You, D., Wang, M. M., and Ye, B. C. (2017). Acetyl-CoA synthetases of *Saccharopolyspora erythraea* are regulated by the nitrogen response regulator GlnR at both transcriptional and post-translational levels. *Mol. Microbiol.* 103, 845–859. doi: 10.1111/mmi.13595
- Zhang, Y. J., and Rubin, E. J. (2013). Feast or famine: the host-pathogen battle over amino acids. *Cell Microbiol.* 15, 1079–1087. doi: 10.1111/cmi.12140
- Zu, H. B. K., Miczak, A., Swenson, D. L., and Russell, D. G. (1999). Characterization of activity and expression of isocitrate lyase in *Mycobacterium avium* and *Mycobacterium tuberculosis*. *J. Bacteriol.* 181, 7161–7167.

Conflict of Interest: The authors declare that the research was conducted in the absence of any commercial or financial relationships that could be construed as a potential conflict of interest.

Copyright © 2021 Qi, She, Du and Ye. This is an open-access article distributed under the terms of the Creative Commons Attribution License (CC BY). The use, distribution or reproduction in other forums is permitted, provided the original author(s) and the copyright owner(s) are credited and that the original publication in this journal is cited, in accordance with accepted academic practice. No use, distribution or reproduction is permitted which does not comply with these terms.